Journal of Energetic Materials
Publication details, including instructions for authors and subscription information:
http://www.informaworld.com/smpp/title~content=t713770432

Inducing Nanoscale Morphology Changes of Pentaerythritol Tetranitrate Using a Heated Atomic Force Microscope Cantilever

Omkar A. Nafday[a]; Brandon L. Weeks[a]; William P. King[b]; Jungchul Lee[b]
[a] Department of Chemical Engineering, Texas Tech University, Lubbock, Texas, USA [b] Department of Mechanical Engineering, University of Illinois, Urbana, Champaign, Illinois, USA

To cite this Article Nafday, Omkar A. , Weeks, Brandon L. , King, William P. and Lee, Jungchul(2009) 'Inducing Nanoscale Morphology Changes of Pentaerythritol Tetranitrate Using a Heated Atomic Force Microscope Cantilever', Journal of Energetic Materials, 27: 1, 1 — 16
To link to this Article: DOI: 10.1080/07370650802328830
URL: http://dx.doi.org/10.1080/07370650802328830

Journal of Energetic Materials, 27: 1–16, 2009

ISSN: 0737-0652 print/1545-8822 online
DOI: 10.1080/07370650802328830

Inducing Nanoscale Morphology Changes of Pentaerythritol Tetranitrate Using a Heated Atomic Force Microscope Cantilever

OMKAR A. NAFDAY,[1] BRANDON L. WEEKS,[1] WILLIAM P. KING,[2] and JUNGCHUL LEE[2]

[1]Department of Chemical Engineering, Texas Tech University, Lubbock, Texas, USA
[2]Department of Mechanical Engineering, University of Illinois, Urbana, Champaign, Illinois, USA

Controlling the morphology of pentaerythritol tetranitrate (PETN) is an important aspect in the nanodetonics research area. Detonation properties are highly dependent on surface area and morphology of PETN. For the first time we show that changes in morphology can be modified at the nanoscale by using a heated atomic force microscope (AFM) cantilever. At temperatures of ∼65°C, faceting of PETN islands is observed, whereas at higher temperatures (∼124°C) the height of the islands decrease by an order of magnitude.

Keywords: atomic force microscope, pentaerythritol tetranitrate, temperature, thermal cantilever

Address correspondence to Brandon Weeks, Texas Tech University, Department of Chemical Engineering, 6th Street and Canton, Lubbock, TX 79409. E-mail: Brandon.weeks@ttu.edu

Introduction

Pentaerythritol tetranitrate (PETN, $C_5H_8N_4O_{12}$) is a crystalline energetic material and one of the strongest known secondary high explosives. It has been the subject of a number of fundamental studies both theoretical [1,2] and experimental, including shock wave-induced decomposition chemistry of PETN crystals and its thermal decomposition properties [3–6]. Since PETN is commonly used in detonatators, the ignitibility and performance can be directly correlated to specific surface area and morphology with nano length scales [7]. In addition to morphology, other nanoscale properties such as voids and defects can dramatically alter the ''hot-spot'' development [8] and the detonation and ignition properties of explosives [9]. Thus, direct measurement techniques are crucial to understanding materials behavior at the nanoscale and may lead to direct engineering to create artificial voids in PETN film in order to tailor energetic material properties [10]. In this work we demonstrate that morphology changes can be observed in PETN at the nanoscale by using a heated cantilever operated on an atomic force microscope (AFM) platform.

The AFM [11] is a versatile tool in research of properties of materials at the nanoscale. The AFM has been used as a tool for nanoscale imaging of a wide range of materials like calcite micro crystals [12] and alumina [13], observing nitride semiconductor defects [14], nanoscale imaging of ferroelectric domains [15], and in the characterization of high-energy nanoparticles [16]. Techniques based on AFM have also been used to study energetic materials, including deflagration studies of explosives [17–19], solid–solid phase transitions in cyclotetramethylene-tetranitramine [20], and the effects of shock on explosives at the nanoscale [21]. The concept of thermal cantilevers is not new [22–24]. These were originally developed as a tool to develop AFM platform–based thermomechanical data writing and reading. The cantilevers were made from doped single-crystal silicon with an integrated differentially doped localized heater region. Detailed studies of the electrical, thermal, and mechanical characterization can be found elsewhere [17,25–27].

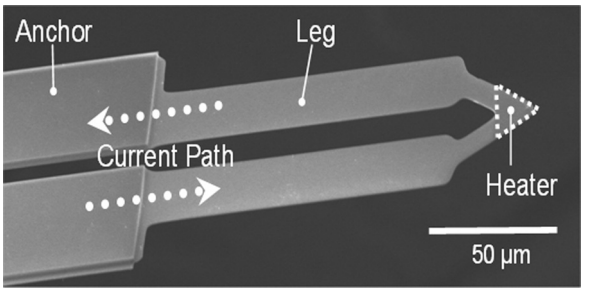

Figure 1. SEM image of a typical thermal cantilever used in the present study.

An SEM image of a thermal cantilever used in this work is shown in Fig. 1. The electronic circuit behind the voltage-driven thermal cantilever assembly consists of a 10-kΩ sense resistor in series with the cantilever to control current flow and avoid damage to the cantilever. The total voltage in the system is distributed between the cantilever and the sense resistor. A voltage is measured across a sense resistor and thus the voltage drop across the cantilever can be calculated. The cantilever resistance increases with the externally applied voltage and since the sense resistance (10 kΩ) is constant, the cantilever is heated resistively. These cantilevers have been demonstrated in the past to deposit polymers [28] and metal nanostructures [29], measure thermally induced material softening [30], and perform high-speed thermochemical nanolithography [31], among other applications.

The ability to control local morphology of materials extends beyond PETN. By locally changing the structure of materials, one can expect a major change in the bulk material properties, most notably the Young's modulus of elasticity, toughness, tear (tear resistance), and rigidity properties. Thus, thermal cantilevers conceivably enable us to tailor the bulk properties of materials, provided that the material in question has a suitable melting/decomposition temperature. Another area of interest might be local ''healing'' of materials that have thermosetting characteristics. Significantly, coarsening, melting, and surface

area investigations of materials like PETN can be performed at the nanoscale. The thermally modified regions could be compared or extrapolated to the physical properties of the bulk material.

Experimental

PETN was evaporated onto freshly cleaned silicon wafers (1 cm × 1 cm). The Si wafers were cleaned thoroughly before use using SC1 ammonia cleaning solution (1:1:5 NH_4OH:-H_2O_2:H_2O parts by volume) at 80°C for ∼10 min [32]. The wafers were subsequently cleaned with deionized water and dried prior to use. These were then mounted upside down on clean glass slides using double-sided tape. PETN crystals were heated on a hotplate with a thermometer–sand bath arrangement to the sublimation temperature of PETN. The cleaned Si wafers were kept above the PETN crystal, with the clean side facing the PETN vapors and the other side of the mounted Si wafers kept cool using a beaker of cold water. This was done to facilitate the PETN vapor condensation on the Si wafer, resulting in stable films. The temperature of the sand bath in which the PETN crystals were kept was monitored and the Si wafers were only introduced after the temperature of the sand bath had reached ∼80°C. Evaporation was carried out for ∼20 min until a thick PETN film coating was visibly observed on the Si wafer.

These PETN films were then allowed to cool further at room temperature for a few hours and were ready for imaging/surface modification with a thermal cantilever already mounted in a special AFM tip holder. The AFM was a Veeco Multimode NanoScope IIIa (Veeco Metrology Inc., Santa Barbara, CA). Special resistively heated AFM cantilevers were fabricated at the University of Illinois (Urbana–Champaign, IL). The AFM was operated under ambient conditions. An external HY 3003 D-3 DC power supply (Precision Mastech, Kowloon, Hong Kong) was used to provide voltage to the thermal cantilevers and a 3456 A digital voltmeter (Hewlett Packard, Palo Alto, CA) was used to check the sense voltage across the 10-kΩ

resistor. Details of the thermal cantilever circuit can be found elsewhere [33]. The heated tip was brought in contact with the evaporated PETN film at a certain voltage (temperature) and scanning was started as soon as reliable feedback was achieved. Figure 2 is a schematic representation of a thermal cantilever reducing the PETN film thickness due to continuous scanning at a certain temperature, whereas at another temperature the film forms faceted edges. The PETN film was scanned continuously at 0.25 Hz (corresponding scan speed is 7.5 μm/s) over the same $15 \times 15\,\mu m^2$ region for a period of ∼4.5 h, with

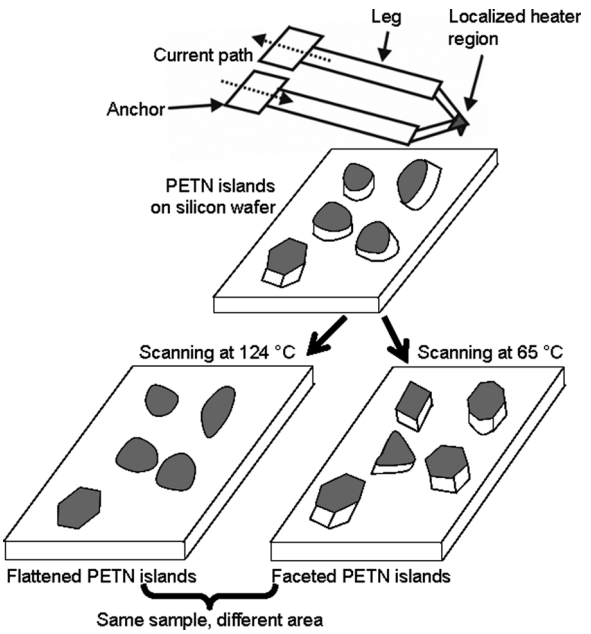

Figure 2. Schematic representation of a thermal cantilever–induced morphology change of PETN film. Continuous scanning at a fixed temperature with a heated cantilever enables control over the final morphology of PETN film. The film morphology is shown to be dependent on cantilever temperature, and by modifying the scanning time, the final PETN film thickness and morphology can potentially be controlled.

continuous collection of PETN film height channel images. Subsequent to image collection, the average PETN island heights and their standard deviations were measured using the histogram analysis tool in the NanoScope V5 image processing software available commercially.

Results and Discussion

The cantilever temperature characterization was performed using the Raman spectroscopy technique [25]. At the different voltages (14 and 16 V), the cantilever resistance was measured to be 1.26 and 1.415 kΩ, respectively, and the cantilever temperature as a function of resistance was plotted as shown in Fig. 3. With a calculated power of 0.733 and 1.626 mW supplied to the cantilever at the two voltages, respectively, the cantilever temperature was measured to be 65 and 124°C, respectively. These temperatures are lower than the expected bulk PETN melting point (140°C) [6]. The selection of scan rate (Hz) during thermal cantilever experiments is crucial since a faster scan will

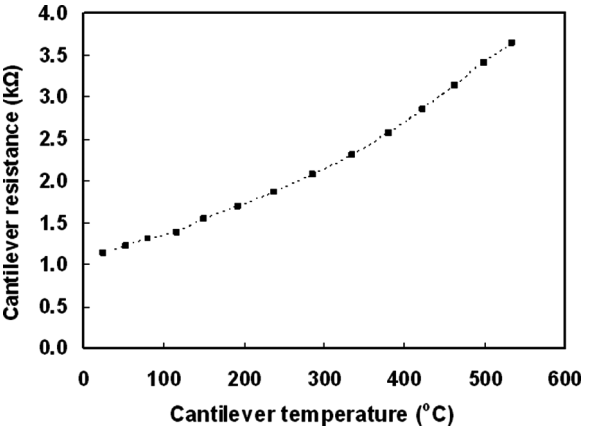

Figure 3. Characterization of the cantilever temperature was performed using Raman I-R by measuring the cantilever temperature as a function of cantilever resistance. The temperature at 14 and 16 V was found to be 65 and 124°C, respectively.

entail a shorter PETN film-hot cantilever contact time. The focus of the current study was to see whether this technique can lead to morphological changes in the PETN film; as such, the selection of the current scan rate (0.25 Hz, 15 μm scan size) was one of the many different (0.125, 0.25, 0.5, 1.0 Hz) scan rates tried. The effect of variation of scan rate on PETN sublimation during contact in a typical thermal cantilever experiment has not received significant attention in recent literature and can be the subject of a separate study.

Figure 4 shows a time progression of PETN film morphology change in the same 15×15 μm area due to continuous scanning of a thermal cantilever at 16 V, 124°C. All images are AFM height channel and were plane-leveled after collection. Compared to Fig. 4a, the film undergoes noticeable lateral flattening as seen

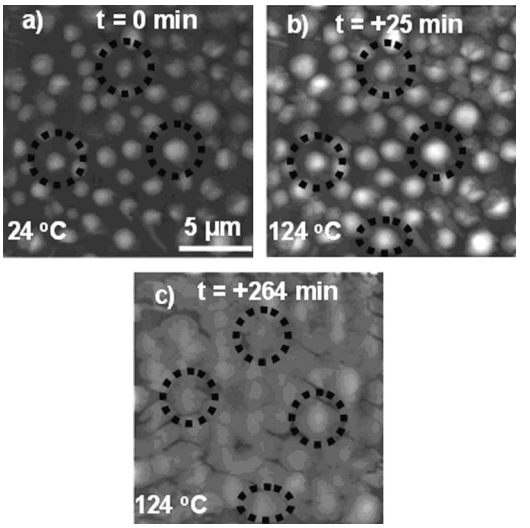

Figure 4. Typical representation of change in PETN film morphology over time: (a) Original PETN film at time zero, with cantilever at 0 V, 24°C; (b) same film after 25 min with cantilever at 16 V, 124°C; (c) after 264 min of scanning with a thermal cantilever at 16 V, 124°C. All images shown are AFM height channel and all images collected are 15×15 μm.

Table 1
Tabulation of the root mean square (RMS) roughness over elapsed time of the PETN film shown in Figures 4 and 5. RMS roughness only decreased for the higher temperature scan results of Figure 4 (124°C)

Figure	Cantilever temperature (°C)	Elapsed time (min)	RMS roughness (nm)	Average island area (μm^2)
4a	24	0	70	1.04
4b	124	25	54	1.42
4c	124	264	20	N/A
5a	24	0	131	0.98
5b	65	34	128	1.06
5c	65	273	123	1.02
5d	65	1450	121	1.28

in Figs. 4b and 4c. The average initial height of the film in Fig. 4a is ~345 nm, but within a period of just 4.5 h, it reduces by an order of magnitude. The root mean square (RMS) roughness of the PETN film is also observed to decrease as shown in Table 1, most likely due to PETN inter-grain boundary smoothening.

In order to test whether the film height reduction was induced only due to the local temperature of the hot cantilever, the temperature (voltage) of the cantilever was reduced. The cantilever was kept at 65°C and moved to a fresh area on the same PETN sample. After tip approach, the hot cantilever was scanned repeatedly over the same area in order to investigate whether the PETN film height decreased due to the hot cantilever scanning. Figures 5a–5d show the time lapse AFM height channel images of the PETN film scanned with the thermal cantilever at 65°C. Figures 5a and 5c represent the initial and final condition of the film after ~4.5 h, respectively. No evidence of film flattening was observed after 4.5 h; the average height was measured to be ~320 nm compared to 350 nm at time = 0. An interesting observation after just 24 h of scanning

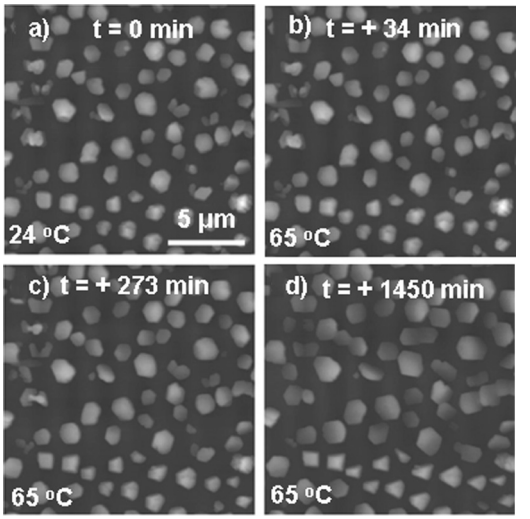

Figure 5. AFM height images of PETN film; all scans are 15 µm. (a) At the start of scan, with cantilever at 0 V, 24°C; (b) after 34 min with cantilever at 14 V, 65°C; (c) after 273 min min with cantilever at 14 V, 65°C; and (d) after 1450 min with cantilever at 14 V, 65°C.

is that the PETN film develops facets as seen in Fig. 5d, becomes decidedly sharp (compare Fig. 5d to Fig. 5a), and starts to flatten out (film height decreased to ∼260 nm).

The line scans of images shown in Figs. 4a–4c and 5a–5c are depicted in Figs. 6a and 6b, respectively, as a function of the background subtracted film heights. The individual x–z film heights measured from the height channel images were divided by the minimum z height among all z film height values, to obtain the background subtracted z values. Diagonal line scans taken across each image at the same locations in Fig. 4 are shown in Fig. 6a. Clear reduction of film height is seen for the image scanned after 264 min (solid dark line in Fig. 6a). Figure 6b shows the line scans of Figs. 5a–5c, where no significant change in film height was observed after a similar scanning time (273 min).

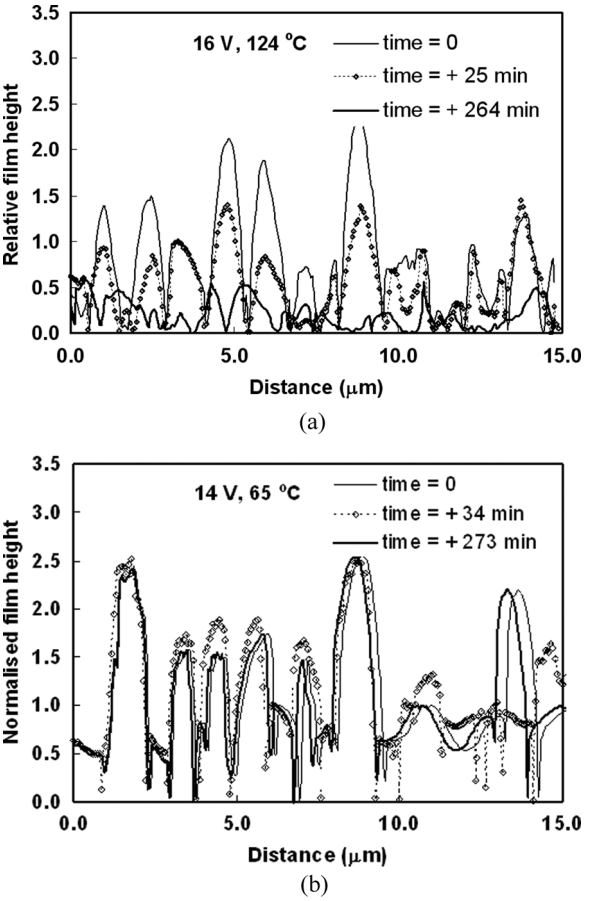

Figure 6. (a) Line scans of Figs. 4a, 4b, and 4c plotted in units of normalized height as a function of elapsed scanning time. Clear reduction in film height is evident after progressive time periods of scanning with the cantilever at 124°C, as shown by the respective lines. (b) In comparison, the line scans of Figs. 5a–5c show no significant reduction in film height.

Figure 7 shows the film height measurements of Figs. 4a–4c and 5a–5c. Only the intermediate elapsed times in the first 5 h of thermal scanning have been shown for clarity and comparison with each other. Error bars represent the standard

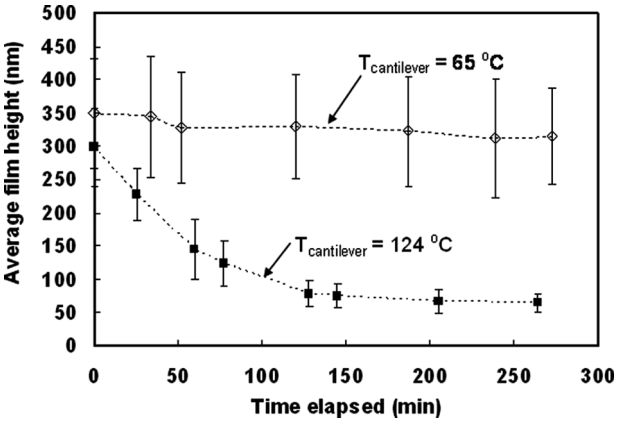

Figure 7. The film heights were monitored over time and found to reduce by almost an order of magnitude after around 4.5 h of scanning with the cantilever at 124°C. However, the film scanned with the cantilever at 65°C in the same time frame showed no significant change in film height. Film height measured after ∼24 h of scanning at 65°C (not shown) was measured to be ∼320 nm. The error bars represent standard deviations of all the island film height measurements using histogram analysis.

deviations of film height measurements, calculated using the histogram analysis function in the NanoScope™ image processing software (Veeco Metrology Inc., Santa Barbara, CA). This reduction in film height was reproducibly observed after moving to a different area on the PETN evaporated film after a similar scan time. The experiment in Fig. 4 (cantilever at 124°C) was stopped after 4.5 h in order to clearly discern the PETN film height compared to the background silicon surface and to feasibly measure the film height.

The above results show that depending on the thermal cantilever selected, changing the cantilever temperature (in this case 59°C), dramatically changes the type of morphology observed at the nanoscale. Moving to a different area and increasing the cantilever temperature to 124°C again led to PETN film

flattening in just over 4.5 h, showing this to be a reproducible result. This also suggests that film flattening is probably independent of the age of the prepared evaporated PETN film, but more thorough investigations are needed to resolve this. The morphological changes observed in Figs. 4 and 5 may also be the result of repeated heating/cooling cycles the PETN film is subjected to. Since each subsequent image takes ~9 min to be collected (15 μm scan at 0.25 Hz), it is plausible to think that the PETN has sufficient time to cool before the hot cantilever comes back to the same area. Thus, the temperature cycling between heat flow to and from the PETN and the heated cantilever can possibly be said to "mold" the PETN along the crystallographic direction of its most favorable energy state [34–36].

Conclusions

This study presents the first experimental evidence of AFM heated cantilever–induced morphological flattening of PETN film by using the cantilever to locally scan over the same region continuously. We demonstrate that the PETN film can be transformed within a relatively short time frame (~4.5 h) to reduce by an order of magnitude in height. Moreover, since the PETN film is only locally modified and the exposure to the heated tip can be controlled, there is no possibility of damage to the PETN film due to bulk sublimation. Other areas of PETN film on the Si wafer are unchanged, leading to local control of PETN film morphology, previously unknown by any other technique. We demonstrate the method of using thermal cantilevers to be potentially applicable for local thin film modification of substances that have melting points similar to PETN and that are within the operating range of thermal cantilevers (up to 1000°C) like other explosives, polymers, and thin metal films.

Acknowledgements

This work was partially supported by the following grants: NSF CAREER (CBET-0644832), ONR N00014-06-1-0922, and ARO W911NF-07-1-0531.

References

[1] Allis, D. G. and T. M. Korter. 2006. Theoretical analysis of the terahertz spectrum of the high explosive PETN. *ChemPhysChem*, 7: 2398–2408.

[2] Byrd, E. F. C. and B. M. Rice. 2007. Ab initio study of compressed 1,3,5,7-tetranitro-1,3,5,7-tetraazacyclooctane (HMX), cyclotrimethylenetrinitramine (RDX), 2,4,6,8,10,12-hexanitrohexaazaisowurzitane (CL-20), 2,4,6-trinitro-1,3,5-benzenetriamine (TATB), and pentaerythritol tetranitrate (PETN). *Journal of Physical Chemistry C*, 111: 2787–2796.

[3] Olinger, B., P. M. Halleck, and H. H. Cady. 1975. Isothermal linear and volume compression of Pentaerythritol tetranitrate (PETN) to 10 GPa (100 kbar) and calculated shock compression *Journal of Chemical Physics*, 62: 4480–4483.

[4] Dreger, Z. A., Y. A. Gruzdkov, Y. A. Gupta, and J. J. Dick. 2002. Shock wave induced decomposition chemistry of pentaerythritol tetranitrate single crystals: Time-resolved emission spectroscopy. *Journal of Physical Chemistry B*, 106: 247–256.

[5] Lee, J. S., C. K. Hsu, and C. L. Chang. 2002. A study on the thermal decomposition behaviors of PETN, RDX, HNS and HMX. *Thermochimica Acta*, 392: 173–176.

[6] Tarver, C. M., T. D. Tran, and R. E. Whipple. 2003. Thermal decomposition of pentaerythritol tetranitrate. *Propellants Explosives Pyrotechnics*, 28: 189–193.

[7] Edmonds, E., A. Hazelwood, T. Lilly, and J. Mansell. 2007. Development of in-situ surface area analysis for detonators. *Powder Technology*, 174: 42–45.

[8] Armstrong, R. W. 1995. Dislocation mechanisms for shock-induced hot-spots. *Journal De Physique IV*, 5: 89–102.

[9] Dlott, D. D. 2006. Thinking big (and small) about energetic materials. *Materials Science and Technology*, 22: 463–473.

[10] King, W. P., S. Saxena, B. A. Nelson, B. L. Weeks, and R. Pitchimani. 2006. Nanoscale thermal analysis of an energetic material. *Nano Letters*, 6: 2145–2149.

[11] Binnig, G., C. F. Quate, and C. Gerber. 1986. Atomic force microscope. *Physical Review Letters*, 56: 930.

[12] Chien, Y. C., A. Mucci, J. Paquette, S. K. Sears, and H. Vali. 2006. Comparative study of nanoscale surface structures of calcite microcrystals using FE-SEM, AFM, and TEM. *Microscopy and Microanalysis*, 12: 302–310.

[13] Gritschneder, S., C. Becker, K. Wandelt, and M. Reichling. 2007. Disorder or complexity? Understanding a nanoscale template structure on alumina. *Journal of the American Chemical Society*, 129: 4925–4928.

[14] Simpkins, B. S., H. Zhang, and E. T. Yu. 2006. Defects in nitride semiconductors: From nanoscale imaging to macroscopic device behavior. *Materials Science in Semiconductor Processing*, 9: 308–314.

[15] Wittborn, J., C. Canalias, K. V. Rao, R. Clemens, H. Karlsson, and F. Laurell. 2002. Nanoscale imaging of domains and domain walls in periodically poled ferroelectrics using atomic force microscopy. *Applied Physics Letters*, 80: 1622–1624.

[16] Mercado, L., P. M. Torres, L. M. Gomez, N. Mina, S. P. Hernandez, R. Lareau, R. T. Chamberlain, and M. E. Castro-Rosario. 2004. Synthesis and characterization of high-energy nanoparticles. *Journal of Physical Chemistry B*, 108: 12314–12317.

[17] Lee, J. and W. P. King. 2007. Microcantilever hotplates: Design, fabrication, and characterization. *Sensors and Actuators A – Physical*, 136: 291–298.

[18] Pinnaduwage, L. A., T. Thundat, A. Gehl, S. D. Wilson, D. L. Hedden, and R. T. Lareau. 2004. Desorption characteristics, of uncoated silicon microcantilever surfaces for explosive and common nonexplosive vapors. *Ultramicroscopy*, 100: 211–216.

[19] Li, D., L. Senesac, and T. G. Thundat. 2008. Speciation of energetic materials on a mircocantilever using surface reduction. *Scanning*, 30: 208–212.

[20] Weeks, B. L., C. M. Ruddle, J. M. Zaug, and D. J. Cook. 2002. Monitoring high-temperature solid-solid phase transition of HMX with atomic force microscopy. *Ultramicroscopy*, 93: 19–23.

[21] Sharma, J., R. W. Armstrong, W. L. Elban, C. S. Coffey, and H. W. Sandusky. 2001. Nanofractography of shocked RDX explosive crystals with atomic force microscopy. *Applied Physics Letters*, 78: 457–459.

[22] King, W. P., T. W. Kenny, K. E. Goodson, G. L. W. Cross, M. Despont, U. T. Durig, H. Rothuizen, G. Binnig, and P. Vettiger. 2002. Design of atomic force microscope cantilevers for combined thermomechanical writing and thermal reading in array operation. *Journal of Microelectromechanical Systems*, 11: 765–774.

[23] King, W. P., T. W. Kenny, K. E. Goodson, G. Cross, M. Despont, U. Durig, H. Rothuizen, G. K. Binnig, and P. Vettiger. 2001.

Atomic force microscope cantilevers for combined thermomechanical data writing and reading. *Applied Physics Letters*, 78: 1300–1302.

[24] Vettiger, P., G. Cross, M. Despont, U. Drechsler, U. Durig, B. Gotsmann, W. Haberle, M. A. Lantz, H. E. Rothuizen, R. Stutz, and G. K. Binnig. 2002. The ''Millipede''—Nanotechnology entering data storage. *IEEE Transactions on Nanotechnology*, 1: 39–55.

[25] Lee, J., T. Beechem, T. L. Wright, B. A. Nelson, S. Graham, and W. P. King. 2006. Electrical, thermal, and mechanical characterization of silicon microcantilever heaters. *Journal of Microelectromechanical Systems*, 15: 1644–1655.

[26] Nelson, B. A. and W. P. King. 2007. Temperature calibration of heated silicon atomic force microscope cantilevers. *Sensors and Actuators A – Physical*, 140: 51–59.

[27] Park, K., J. Lee, Z. M. M. Zhang, and W. P. King. 2007. Frequency-dependent electrical and thermal response of heated atomic force microscope cantilevers. *Journal of Microelectromechanical Systems*, 16: 213–222.

[28] Yang, M., P. E. Sheehan, W. P. King, and L. J. Whitman. 2006. Direct writing of a conducting polymer with molecular-level control of physical dimensions and orientation. *Journal of the American Chemical Society*, 128: 6774–6775.

[29] Nelson, B. A., W. P. King, A. R. Laracuente, P. E. Sheehan, and L. J. Whitman. 2006. Direct deposition of continuous metal nanostructures by thermal dip-pen nanolithography. *Applied Physics Letters*, 88(3): 033104.

[30] Nelson, B. A. and W. P. King. 2007. Measuring material softening with nanoscale spatial resolution using heated silicon probes. *Review of Scientific Instruments*, 78(2): 023702–023702-8.

[31] Szoszkiewicz, R., T. Okada, S. C. Jones, T. D. Li, W. P. King, S. R. Marder, and E. Riedo. 2007. High-speed, sub-15 nm feature size thermochemical nanolithography. *Nano Letters*, 7: 1064–1069.

[32] Kern, W. and D. A. Puotinen. 1970. Cleaning solutions based on hydrogen peroxide for use in silicon semiconductor technology. *RCA Review*, 31: 187–206.

[33] King, W. P. 2005. Design analysis of heated atomic force microscope cantilevers for nanotopography measurements. *Journal of Micromechanics and Microengineering*, 15: 2441–2448.

[34] Cady, H. H. and A. C. Larson. 1975. Pentaerythritol Tetranitrate II: Its crystal structure and transformation to PETN I—An algorithm for refinement of crystal structures with poor data. *Acta Crystallographica Section B-Structural Science*, 31: 1864.

[35] Gruzdkov, Y. A. and Y. M. Gupta. 2001. Vibrational properties and structure of pentaerythritol tetranitrate. *Journal of Physical Chemistry A*, 105: 6197–6202.

[36] Zepeda-Ruiz, L. A., A. Maiti, R. Gee, G. H. Gilmer, and B. L. Weeks. 2006. Size and habit evolution of PETN crystals—A lattice Monte Carlo study. *Journal of Crystal Growth*, 291: 461–467.